Inserting curved boundary layers for viscous flow simulation with high-order tetrahedra

Abel Gargallo-Peiró[1], Xevi Roca[2], Josep Sarrate[1], Jaime Peraire[2]

[1] Laboratori de Càlcul Numèric (LaCàN),
Universitat Politècnica de Catalunya, Barcelona 08034, Spain
{abel.gargallo,jose.sarrate}@upc.edu

[2] Department of Aeronautics and Astronautics,
Massachusetts Institute of Technology, Cambridge, MA 02139, USA
{xeviroca,peraire}@mit.edu

1 Introduction

We propose an *a posteriori* approach for generating curved meshes for viscous flow simulations composed by high-order tetrahedra. The proposed approach is performed in the following three steps: (1) generate a linear tetrahedral mesh for inviscid flow; (2) insert a boundary layer mesh, composed by linear tetrahedra, on the viscous part; and (3) convert the linear tetrahedral mesh to a curved and high-order mesh for viscous flow. This approach provides high-order tetrahedral meshes with boundary layer parts that are composed by elements that are: curved, valid, and of any interpolation degree.

The main application of the obtained meshes is the simulation of viscous flow with high-order unstructured solvers. Since the obtained meshes are conformal and fully composed by tetrahedra, they can be used with any continuous and discontinuous Galerkin solver that features linear and high-order tetrahedra. That is, it does not require a solver for non-conformal and hybrid meshes. To show the applicability of the method, we present the flow around a curved geometry obtained with the hybridized discontinuous Galerkin method.

2 Methodology and application: flow around a sphere

In this section, we outline the proposed method and we apply it to generate a mesh for the simulation of the viscous flow around a sphere. Note that a high-fidelity approximation of the flow requires a curved and high-order mesh with an anisotropic boundary layer in the regions adjacent to the sphere. The geometry of the sphere is described *exactly* (up to machine accuracy) by a 3D CAD model composed by 8 NURBS surfaces of degree 3 that correspond to

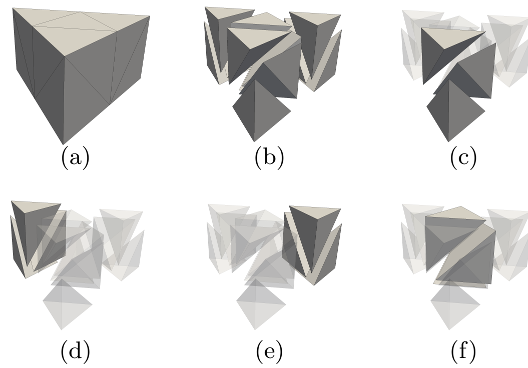

Fig. 1. Template for a prism defined by an extruded triangle on the wall boundary.

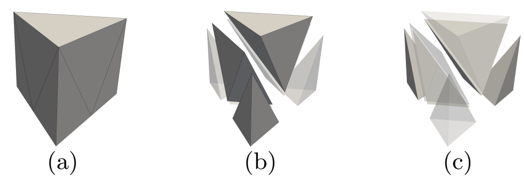

Fig. 2. Template for a prism connecting the viscous and inviscid parts of the mesh.

the sphere octants. The rest of the mesh can be isotropic and corresponds to the inviscid part of the flow.

To illustrate the method, below we describe the meshes obtained in the different steps. Specifically, all the elements are colored according to a measure of the quality respect an ideal element [1], see Figure 3. This quality measure is also used to obtain the mesh statistics, see Table 1. Furthermore, the reciprocal of the quality (distortion) is minimized to smooth and untangle the inserted elements on the viscous part, see reference [1] for details. Note that this node relocation approach approach is an alternative to existent curved boundary layer meshing methods based on topological modifications [2]. Finally, we present a high-order approximation of the flow around the curved mesh of a sphere. The flow is obtained with a parallel implementation of the hybridized discontinuous Galerkin method [3].

1. Generate a linear tetrahedral mesh for inviscid flow. The first step in our methodology is to generate an isotropic linear mesh for inviscid flow simulations. The mesh has to be finer in the regions of higher curvature, and has to provide the required resolution on the inviscid part. Specifically, the inviscid mesh for the sphere is composed by 18936 linear tetrahedra and 3753 points, Figure 3(a). All the elements have quality one, since this initial mesh is considered the ideal mesh for the inviscid part.

2. Insertion of the boundary layer in the viscous part. The goal of this step is to obtain a valid linear mesh for viscous flow simulations. This step is performed in two stages: i) insert a linear boundary layer; and ii) smooth and untangle the initial viscous linear mesh.

First, we insert the topology of the boundary layer. To this end, we generate a layer of prisms by extruding in the normal direction the triangles on the wall boundary. The extrusion distance is the ten percent of the final desired boundary layer height since the goal is just to obtain the mesh topology. Then, the inserted layer is converted to a boundary layer mesh by splitting each prism in several levels of tetrahedra. The number of levels is characterized by: an initial size on the normal direction, the growing factor of the size along the normal direction, and a final size. To split the inserted layer, we consider two templates to split a prism in tetrahedral elements. The first template (Figure 1) is composed by 12 tetrahedra, and it is stacked along the normal direction, starting from the wall boundary, to form the boundary layer. The second template (Figure 2) is composed by 7 tetrahedra, and is used to connect the last layer of the viscous part of the mesh with the first layer of the inviscid part. Both templates ensure that the obtained mesh is conformal. Note that the triangles of the wall boundary have to be split into four triangles to insert the boundary layer. The boundary layer topology is composed by 24986 elements. This results in a viscous mesh composed by a total of 43922 elements and 8595 points. Note that the inserted tetrahedra have lower quality than the ones on the inviscid part, see Figure 3(b).

Second, we smooth and untangle the mesh with the inserted boundary layer. The goal of this step is to obtain a valid and high-quality viscous mesh. The elements on the viscous part have to present the desired stretching, and the elements on the inviscid part have to resemble the mesh size features of the initial linear mesh. To this end, we assign a different ideal element to each element of the mesh. One the one hand, each element on the viscous part is idealized by a tetrahedron that presents the proper stretching along the normal direction to the wall boundary. On the other hand, the elements on the inviscid part are idealized by the corresponding initial linear element. Then, we minimize the distortion respect the assigned ideal mesh using the smoothing and untangling procedure proposed in [1]. This results in a valid tetrahedral mesh with an inserted boundary layer of the proper size and stretching, see Figure 3(c).

3. Conversion to a curved and high-order tetrahedral mesh. In this step, the valid viscous mesh is converted to a curved and high-order tetrahedral mesh. This process is also composed by two stages: i) convert the whole mesh to a high-order mesh; and ii) smooth and untangle the viscous high-order mesh.

First, the linear tetrahedral mesh with the inserted boundary layer is curved and converted to a high-order mesh. To this end, all the straight-sided elements of the mesh are expressed in terms of element-wise polynomials of degree four. Then, the nodes that correspond to faces on the wall boundary

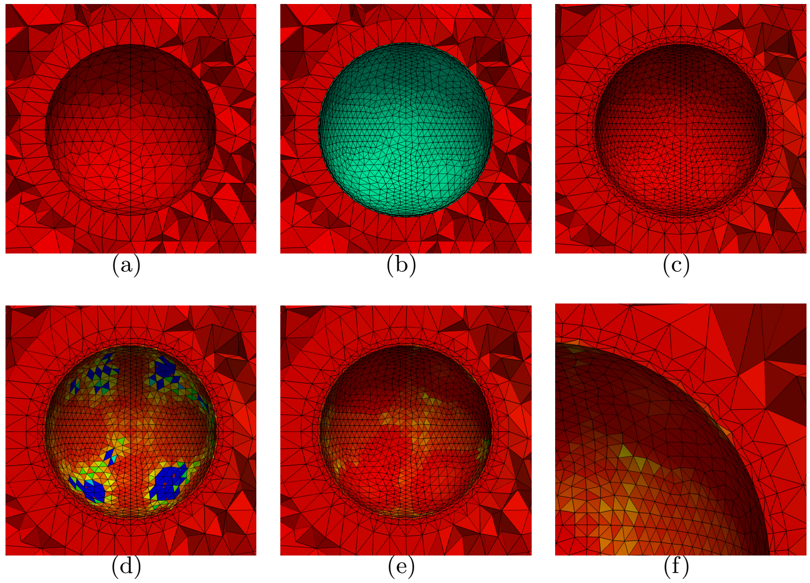

Fig. 3. Shape quality along the process. (a) Inviscid linear mesh. Viscous linear mesh: (b) inserted boundary layer topology, and (c) smoothed and untangled mesh. Viscous mesh of interpolation degree 4: (d) curved wall boundary, (e) smoothed and untangled mesh, and (f) detail of the curved and high-order boundary layer.

Table 1. Shape quality statistics of the meshes presented in Figure 3.

Degree	#elems	#nodes	Fig.	Min.Q.	Max.Q.	Mean Q.	Std.Dev.	#Tang.Elems.
1	18936	3753	3(a)	1.00	1.00	1.00	0.00	0
1	43922	8595	3(b)	0.32	1.00	0.61	0.34	0
1	43922	8595	3(c)	0.97	1.00	1.00	0.00	0
4	43922	487082	3(d)	0.00	1.00	0.98	0.09	311
4	43922	487082	3(e)	0.44	1.00	0.99	0.02	0

are forced to be on the sphere. This results in a curved and high-order mesh with 311 non-valid elements close to the wall boundary, see Table 1.

Second, we repair these invalid elements and increase the mesh quality by using again the smoothing and untangling procedure. It is important to highlight that now the ideal mesh is represented by the viscous linear mesh. The result is a valid curved mesh composed by 43922 valid tetrahedra of interpolation degree 4 and 487082 points, see Table 1. Note that the elements that compound the boundary layer are curved and present the desired anisotropy, see Figures 3(d) and 3(e).

4. Simulation of the viscous flow around a sphere. Finally, the obtained curved and high-order tetrahedral mesh has been used to obtain a high-order approximation of the flow around a sphere of diameter one. Specifi-

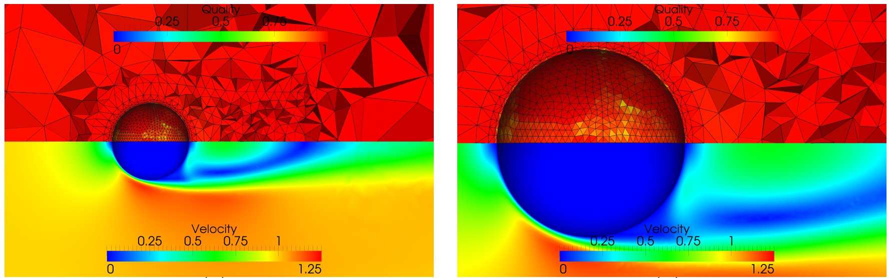

(a) (b)

Fig. 4. Section of the curved mesh of interpolation degree 4 showing the flow velocity and the element quality: (a) general view; and (b) detailed view.

cally, we consider the compressible Navier-Stokes solution for the steady-state flow around a sphere at a Reynolds number of Re $= 200$, and a free-stream Mach number of $M_\infty = 0.3$. Figures 4(a) and 4(b), present an approximation of the velocity magnitude around the sphere with element-wise polynomials of degree four together with the quality of the curved mesh.

3 Concluding remarks

We have presented an *a posteriori* approach for generating curved high-order tetrahedral meshes for viscous flow simulations. The approach provides high-order meshes that include a boundary layer mesh composed by tetrahedra that are: curved, valid, and of any interpolation degree. Moreover, the approach enables the construction of a Navier-Stokes boundary layer mesh (viscous) from an isotropic Euler mesh (inviscid). The main application of this method is to compute with high-fidelity the flow around curved objects. That is, the curved and high-order boundary layer mesh allows the proper representation of the viscous features of the flow close to the wall conditions.

References

1. A. Gargallo-Peiró, X. Roca, J. Peraire, and J. Sarrate. Defining quality measures for validation and generation of high-order tetrahedral meshes. In *22nd International Meshing Roundtable*, 2013.
2. O. Sahni, X.J. Luo, K.E. Jansen, and M.S. Shephard. Curved boundary layer meshing for adaptive viscous flow simulations. *Finite Elements in Analysis and Design*, 46(1):132–139, 2010.
3. X. Roca, N.C. Nguyen, and J. Peraire. Scalable parallelization of the hybridized discontinuous Galerkin method for compressible flow. In *21st AIAA Computational Fluid Dynamics Conference*, 2013.